THE OPTIMIZATION OF A RESONANT TWO-INDUCTOR BOOST CELL FOR A PHOTOVOLTAIC MODULE INTEGRATED CONVERTER

Quan Li* and Peter Wolfs*

*Central Queensland University

Abstract

This paper studies the optimization of a resonant two-inductor boost cell for a photovoltaic (PV) Module Integrated Converter (MIC). The resonant two-inductor boost cell is current fed from a two-phase buck converter and produces a rectified sinusoidal output voltage that is applied to an unfolding stage. This paper concentrates on resonant parameter selection to achieve the lowest power loss. The resonant two-inductor boost cell also employs a resonant gate drive, which minimizes the gate drive power and further improves the converter overall efficiency. The experimental results of a 1 MHz converter with an average power of 50 W are provided.

1. INTRODUCTION

The two-inductor boost converter has been previously developed as the DC-DC conversion stage in the Module Integrated Converter (MIC) for grid interactive photovoltaic (PV) applications, [1]. In this earlier work a hard-switched converter was used to boost low DC voltage from the solar panel to a high DC voltage suitable for conversion to a grid compatible AC voltage. However, a severe disadvantage of the hard-switched two-inductor boost converter is its inability to operate at high switching frequencies while maintaining acceptable efficiencies. To combat the high switching losses under high frequency operation, the resonant two-inductor boost converter has been developed to accomplish the DC-DC conversion in a MIC, as shown in Figure 1, [2]. Unlike the hard-switched two-inductor boost converter, the soft-switched converter is capable of actively utilizing the transformer leakage inductance and the mosfet output capacitance. Therefore, the converter is able to operate under high switching frequencies with a theoretical zero switching loss.

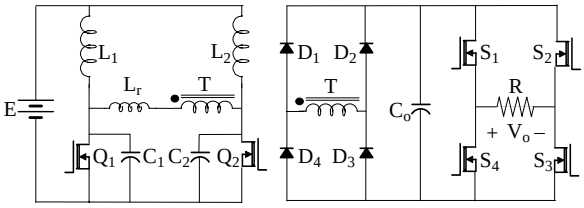

Figure 1. The Resonant Two-Inductor Boost Converter with an Inverter

In Figure 1, the DC link between the boost converter and the full bridge inverter provides a fixed voltage. Therefore the DC-AC inverter requires the Pulse-Width Modulation (PWM) control to generate grid inter-connectable sinusoidal waveforms. This introduces additional losses and it does need relatively complex circuitry, [3].

This paper presents the resonant two-inductor boost converter, where the boost stage cell is fed by the current source from a two-phase synchronous buck converter through an interphase transformer, as shown in Figure 2. The proposed resonant two-inductor boost converter produces a variable DC link with the rectified sinusoidal waveforms and this reduces the following DC-AC inverter to an unfolder with a simple square-wave control.

This paper concentrates on the optimization of the resonant two-inductor boost cell to minimize the total power loss in the cell. Major variable power loss components in the cell are identified and the explicit equations are established. The average of the total variable power loss in the cell is analysed against the circuit parameters numerically. The resonant gate drive circuit is also employed in the converter to reduce the gate drive power under high switching frequencies. Finally, the experimental results of a 50 W converter with 20 V input, 240 V RMS output, operating at 1 MHz are provided.

2. THE CURRENT FED RESONANT TWO-INDUCTOR BOOST CONVERTER

The resonant version of the two-inductor boost converter can operate with variable output voltage using variable frequency control, [4]. However, as the converter is the dual topology to the buck-derived half bridge converter, [5], the achievable output voltage does not reach zero voltage. Another disadvantage of this approach is that the variable frequency control makes the optimized design of the magnetic devices very difficult, [6].

To achieve a wide output voltage range including zero voltage for the resonant two-inductor boost converter, a step-down stage must be introduced. A two-phase synchronous buck converter with an interphase transformer is used as the current source for the resonant boost cell. This approach doubles the

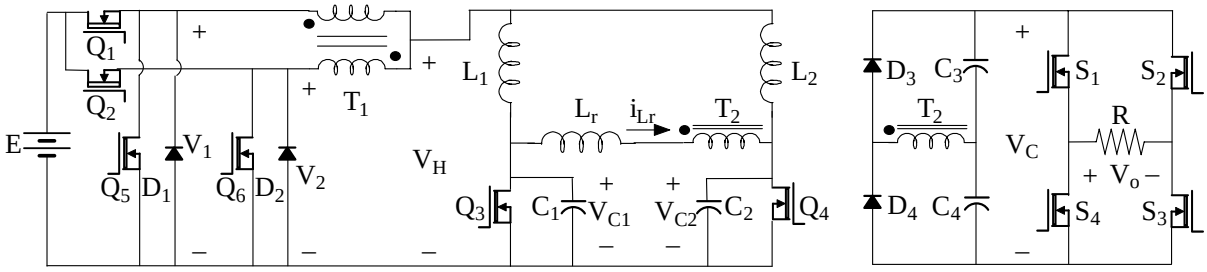

Figure 2. The Resonant Two-Inductor Boost Cell with a Two-Phase Synchronous Buck Rectifier

switching frequency of the buck conversion stage enabling the hard-switched buck converters to avoid the penalty of higher switching losses.

For symmetrical operation of the boost cell, the equivalent switching frequency of the buck conversion stage must be greater than or equal to the switching frequency of the resonant cell. The ratio of the two frequencies is preferentially an integer. Otherwise, the drain source voltage waveforms of the two mosfets will vary and different voltage stresses will occur. Practically, the switching frequency of buck stage mosfets is half of that of the boost stage mosfets as high switching frequencies reduce the efficiency of the hard-switched buck converter. A bonus is that the gate signals of the buck converter mosfets can be easily synchronized through a frequency divider to the control circuit of the boost cell.

The two-inductor boost cell can absorb the parasitic components such as the transformer leakage inductance and the mosfet output capacitance into the resonant tank made up of the inductor L_r and the capacitors C_1 and C_2. Zero-Voltage Switching (ZVS) can be achieved, [2], and theoretically the switching loss can be completely removed. Three important analysis parameters are marked in the resonant waveforms of one operation mode shown in Figure 3. The load factor k is defined by $I_0 \cdot Z_0 = k \cdot V_d$ and k must be greater than or equal to 1 to maintain the ZVS condition, where I_0 is the input current in each inductor in the resonant cell, Z_0 is the characteristic impedance of the resonant tank and V_d is the output voltage reflected to the transformer primary. The timing factor Δ_1 determines the initial inductor current $i_{Lr}(\omega_0 t_0) = \Delta_1 \cdot I_0$ when the mosfet turns off. The initial inductor current is zero in the mode shown in Figure 3. The delay angle α_d is the angle between the instant when the inductor current falls to zero and the instant when the corresponding mosfet turns off in the discontinuous mode, which are respectively shown as $\omega_0 t'$ and $\omega_0 t''$ in Figure 3. According to the definitions of the circuit parameters, only two combinations of the possible domains for k, Δ_1 and α_d exist as shown in Table 1.

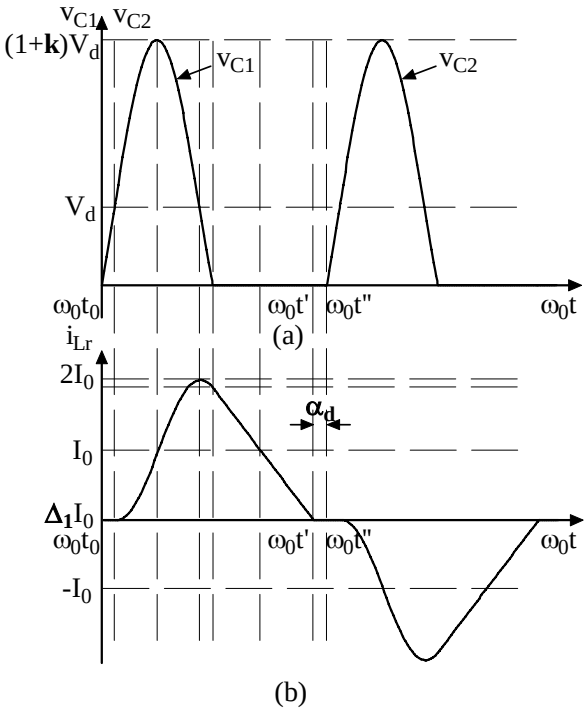

Figure 3. Resonant Waveforms in the Discontinuous Mode (a) Capacitor Voltage (b) Inductor Current

	Region 1	Region 2
k	≥ 1	≥ 1
Δ_1	0	≥ 0
α_d	≥ 0	0

Table 1. Possible Operating Regions

As the boost cell is fed from the sinusoidally modulated buck converter, different mosfet peak drain source voltages occur. In order to maintain the ZVS condition over a low frequency cycle, some attention must be paid to the nonlinearity of the mosfet output capacitance as it varies with the drain source voltage, [7]. The mosfet output capacitance will not be dominant unless the switching frequency is in the range of tens of megahertz, where no additional capacitance is required, [8]. This issue can be avoided if the switching frequency of the resonant converter is below a few megahertz.

In the conventional mosfet gate drive circuit, the drive power loss is proportional to the switching frequency, [9]. Drive power will become a significant portion of the total power loss when the switching frequency is high and this reduces the overall efficiency remarkably. A resonant gate drive, with theoretical zero drive power loss is applied. It requires two pairs of N and P type control mosfets connected in the totem-pole arrangement to provide the drive signal and one additional inductor between mosfets Q_3 and Q_4 to transfer the energy in the gate capacitance in a lossless manner, [10].

3. THE OPTIMIZATION OF THE RESONANT TWO-INDUCTOR BOOST CELL

As the electrical characteristics of the mosfet, the additional resonant inductor and the additional resonant capacitor are pre-determined, the power losses related to these components vary against different circuit parameters. The construction of the transformer is relatively flexible and this allows the design to be carried out after the circuit parameters are selected. The major variable power loss components in the resonant two-inductor boost cell are:

- The power loss in the two mosfets p_Q :

$$p_Q = 2(I_{Q,rms}^2 \cdot R_{DS(on)} + I_{Q,avg} \cdot V_F) \quad (1)$$

where $I_{Q,rms}$ is the effective forward current in the mosfet, $R_{DS(on)}$ is the mosfet forward resistance, $I_{Q,avg}$ is the average reverse current in the mosfet and V_F is the forward drop of the mosfet reverse body diode.

- The power loss in the resonant inductor p_{Lr} :

$$p_{Lr} = I_{Lr,rms}^2 \cdot R_{Lr} \quad (2)$$

where $I_{Lr,rms}$ is the effective current in the resonant inductor and R_{Lr} is the series DC plus AC resistance of the resonant inductor. The actual power loss in the resonant inductor may be slightly lower than the calculated value from Equation 2 as the transformer leakage inductance forms part of the resonant inductance and the power loss of the series resistance in the transformer model is classified as copper loss.

- The power loss in the two capacitors p_{Cr} :

$$p_{Cr} = 2I_{Cr,rms}^2 \cdot R_{Cr} \quad (3)$$

where $I_{Cr,rms}$ is the effective current in the resonant capacitor and R_{Cr} is the Equivalent Series Resistance (ESR) of the capacitor.

The total power loss p_t which alters with the operating conditions in the resonant cell is:

$$p_t = p_Q + p_{Lr} + p_{Cr} \quad (4)$$

As the input voltage of the cell is modulated sinusoidally, the circuit parameters need to be optimized against the average loss, P_{avg}, over a low frequency sinusoidal cycle. The process can be performed numerically with the MATLAB. The effective forward current and the average reverse current in the mosfet and the effective currents in the resonant inductor and capacitors can be calculated through the state analysis of the equivalent resonant circuit. However, the series DC plus AC resistance of the resonant inductor and the ESR of the resonant capacitor are not directly derived. Instead, the state analysis gives the product of the angular resonant frequency of the resonant tank, ω_0, and the switching period of the resonant cell, T_{boost}, and the characteristic impedance of the resonant tank, in Equations 5 and 6:

$$\gamma = \omega_0 \cdot T_{boost} \quad (5)$$

$$Z_0 = \frac{k \cdot V_d}{I_0} \quad (6)$$

The definitions of the series DC plus AC resistance of the inductor, the ESR of the capacitor and the characteristic impedance of the tank are respectively:

$$R_{Lr} = \frac{2\pi f_{boost} L_r}{Q} \quad (7)$$

$$R_{Cr} = \frac{DF}{2\pi f_{boost} C_r} \quad (8)$$

$$Z_0 = \sqrt{\frac{L_r}{C_r}} = \omega_0 L_r = \frac{1}{\omega_0 C_r} \quad (9)$$

where f_{boost} is the switching frequency of the resonant cell, L_r is the resonant inductance, $C_1 = C_2 = C_r$ is the resonant capacitance, Q is the quality factor of the resonant inductor and DF is the dissipation factor of the resonant capacitor. Manipulations of the Equations (5) to (9) give:

$$R_{Lr} = \frac{2\pi \cdot Z_0}{Q \cdot \gamma} \quad (10)$$

$$R_{Cr} = \frac{DF \cdot \gamma \cdot Z_0}{2\pi} \quad (11)$$

In the calculation of the average power loss in the resonant two-inductor boost cell, the following important parameters are used and they correspond to the components listed in the due course:

- $R_{DS(on)} = 0.027\ \Omega$,
- $V_F = 1.5\ V$,
- $Q = 123$ at 500 kHz,
- $DF = 1/6000$ at 500 kHz.

Figures 4 and 5 respectively shows the surface of the average power loss $P_{avg,\Delta}$ in Region 2 and $P_{avg,\alpha}$ in Region 1 in the resonant boost cell at a 500 kHz device switching frequency or a 1MHz converter frequency. For Region 2, the lowest average power loss occurs when $k = 1$ and $\Delta_1 = 0$, which is 0.66 W. For Region 1, it can be shown that the average power loss can be further lowered.

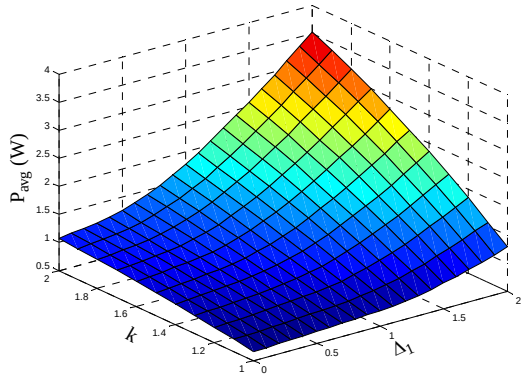

Figure 4. Surface $P_{avg,\Delta}$

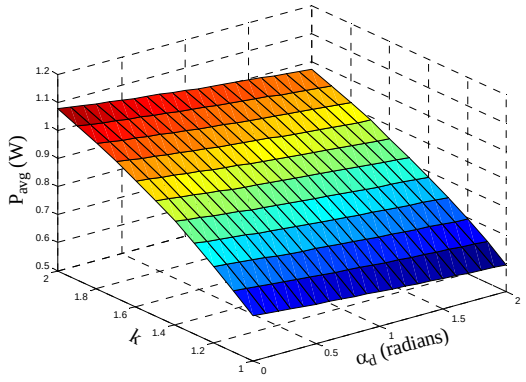

Figure 5. Surface $P_{avg,\alpha}$

Figure 5 shows that the greater α_d, the lower the average power loss under the same k value but the higher the peak switch voltage, which is visually displayed by the surface $V_{peak,\alpha}$ shown in Figure 6. It is better to keep the peak switch voltage below 100 V to obtain a lower mosfet forward resistance. Mosfet input capacitance increases considerably if the same value of the forward resistance is sought under a higher voltage rating, as the product of the mosfet input capacitance and the forward resistance increases with the specified drain-source voltage rating, [11]. A larger mosfet input capacitance either demands a higher power from the conventional drive circuit or causes higher current flowing through the additional inductor in the resonant drive circuit proposed in [10] and this lowers the overall efficiency.

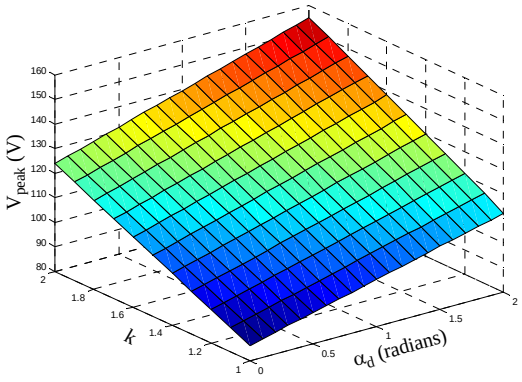

Figure 6. Surface $V_{peak,\alpha}$

Another reason to choose a lower α_d value is that the gradient of the surface $P_{avg,\alpha}$ along the α_d axis is very small. A change in α_d from 0 to 2 when $k = 1$ only results in a power loss decrease of 0.06 W. It is also safe to choose k to be slightly greater than 1 to maintain the ZVS operating condition under any unforseen input disturbances or component tolerance. The final parameters are selected to be $k = 1.1$, $\Delta_1 = 0$ and $\alpha_d = 0$ and the average power loss is 0.72 W. At this operating point, the peak switch voltage is 90 V. Numerical results show that the increase of k from 1 to 1.1 only raises the average power loss by 0.06 W. For an average power output of 50 W, once the circuit parameters are determined, other important values in designing the resonant cell can be obtained as the following:

- Resonant inductance $L_r = 2.80\ \mu H$,
- Resonant capacitance $C_r = 7.85\ nF$,
- Transformer primary to input voltage gain $V_d / V_H = 2.15$.

4. THE CONTROL LOOP IN THE TWO-PHASE BUCK CONVERTER

A Linear Technology two-phase synchronous step-down switching regulator LTC1929 is used to provide driving signals to two phase shifted synchronous buck converters and employs the peak current mode control to ensure current sharing between two phases, [12]. As the controller is designed to produce a fixed output voltage between 0.8 V to 6 V, an external operational amplifier must be added if a variable output with higher peak voltage is targeted. A simplified control diagram is given in Figure 7, where the functional blocks within the dashed line rectangle are implemented internally by the LTC1929. A rectified sinusoidal waveform is used as the demand signal. The buck converter mosfet drain currents are sensed via current transformers and fed back to the

differential current comparators. Slope compensation is used to remove the inherent instability under peak current control with duty ratios greater than 50%, [13]. The Bode plots for transfer functions of the on-chip voltage error amplifier and the external voltage feedback loop are also given in Figure 7.

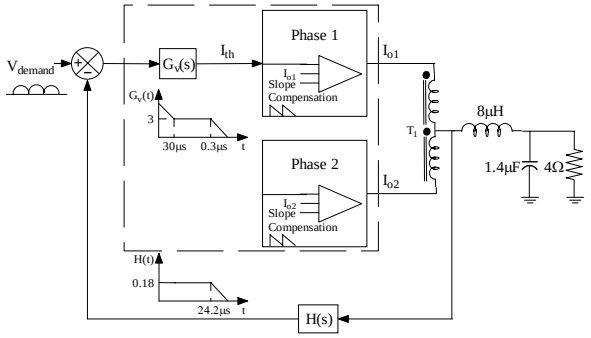

Figure 7. Two-Phase Synchronous Buck Converter Control Block Diagram

5. EXPERIMENTAL WAVEFORMS

The switching frequency of the buck stage mosfets f_{buck} and that of the boost stage mosfets f_{boost} are respectively $f_{buck} = 250\ kHz$ and $f_{boost} = 500\ kHz$. The main components used in the resonant two-inductor boost cell are:

- Inductors L_1 and L_2, and transformer T_2 – Core type Ferroxube ETD29 with 0.5 mm air gap in the two outer legs, ferrite grade 3F3; inductor winding 14 turns; transformer primary - 14 turns of Litz wire made up of 50 strands, secondary - 56 turns of Litz wire made up of 6 strands, primary leakage inductance 0.40 µH.
- Boost converter mosfet – ST STB50NE10, $V_{DS} = 100\ V$, $I_D = 50\ A$, $R_{DS(on)} = 0.027\ \Omega$, $C_{oss} = 0.675\ nF$;
- Resonant capacitor – Cornell Dubilier surface mount mica capacitor MC22FA202J, $C = 2\ nF$, $V_{dc} = 100\ V$, $DF = 1/6000$ at 500 kHz; 7 nF additional resonant capacitance;
- Resonant inductor – 4 of 10µH Miniature radial inductors in parallel, $Q = 123$ at 500 kHz;
- Rectifier diode – STTA106U, $I_F = 1.0\ A$, $V_{RRM} = 600\ V$, $V_F = 1.5\ V$, $t_{rr} = 20\ ns$;
- Rectifier capacitor – 2 pairs of 4 parallel connected Phycomp class X7R multilayer ceramic surface mount capacitor, $C = 0.022\ \mu F$, $V_{dc} = 200\ V$.

Figures 8 to 11 show the experimental waveforms. Figure 8 shows the two-inductor boost converter output V_C and the input V_H from top to bottom during sinusoidal modulation. A three-level modulation can be obviously observed in the V_H waveform although the waveform captured by the oscilloscope is heavily aliased. Figure 9 shows the gate waveforms of the low frequency unfolder switches S_2 (S_4), S_1 (S_3) and the output voltage V_O from top to bottom.

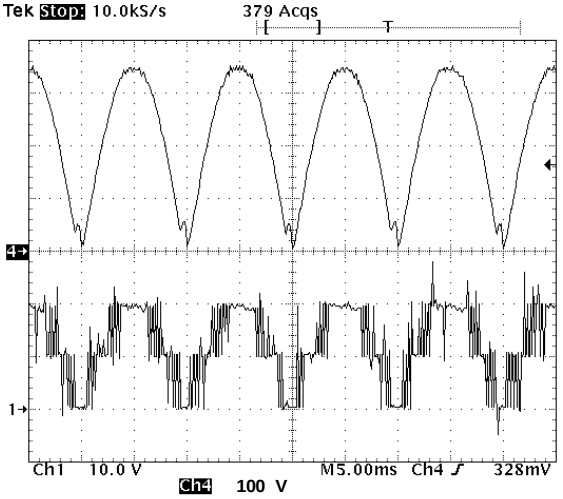

Figure 8. Sinusoidal Modulation Waveforms

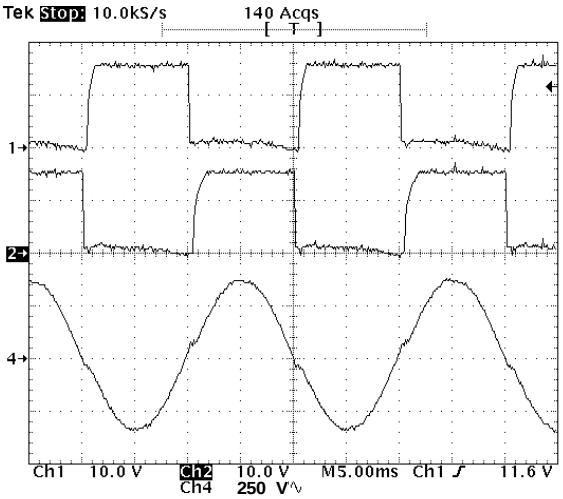

Figure 9. Low Frequency Unfolder Waveforms

From top to bottom, Figure 10 shows the gate and drain voltage waveforms of the mosfets in the two-inductor boost cell close to the peak output voltage point. Compared with the conventional gate drive waveforms, those of the resonant gate drive show a relatively slow transition from zero to positive rail or vice versa. Gate charge energy is transferred losslessly from one mosfet gate capacitance to the other through an inductor lying in between. The mosfet drain waveforms show that the mosfets turn on at zero voltage and the mosfets operate at ZVS. Figure 11 shows the voltage across the diode in the voltage doubler close to the peak output voltage point. No reverse recovery can be seen in the waveform although some oscillations between the diode junction

capacitance and the transformer leakage inductance occur. Normal fast recovery diodes survive in this 340V, 1 MHz application as the semi-sinusoidal current in the transformer primary relaxes the requirement on the reverse recovery.

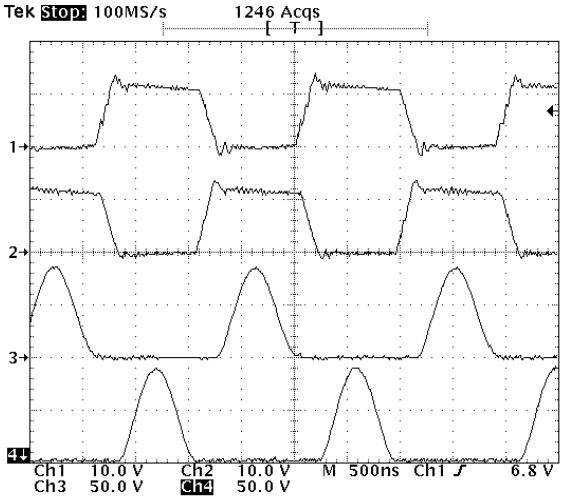

Figure 10. Mosfets Gate and Drain Voltages in the Resonant Two-Inductor Boost Converter

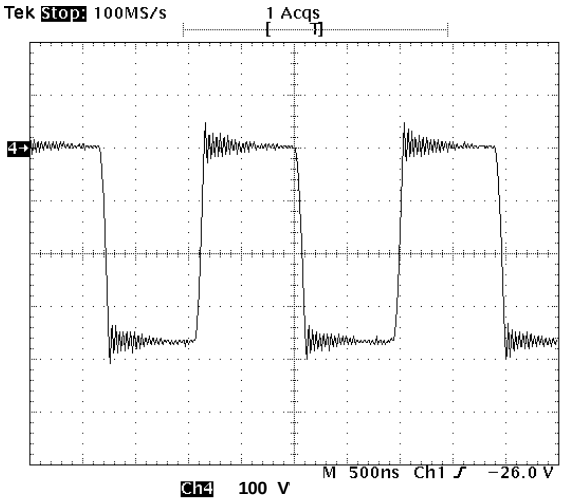

Figure 11. Diode Voltage in the Resonant Two-Inductor Boost Converter

6. CONCLUSIONS

This paper studies the resonant two-inductor boost converter fed from a buck stage converter and especially focuses on the optimization of the variable power loss components in the boost cell. The average total variable power loss is examined quantitatively and an optimizing operating point is determined. In the design of the resonant boost cell, the resonant gate drive and the resonant components with high quality factors are also used to minimize the overall power loss. The experimental results of a 1 MHz 50 W converter are provided and show an overall converter efficiency greater than 90%. It is expected that employing more sophisticated control circuit for the resonant boost cell will further reduce the control power and improve the converter efficiency.

7. REFERENCES

[1] Q. Li, P. Wolfs, S. Senini, "The Application of the Half Bridge Dual Converter to Photovoltaic Applications", *Proc. AUPEC, 2000*, pp. 156-161.

[2] Q. Li and P. Wolfs, "A Resonant Half Bridge Dual Converter," *Proc. AUPEC, 2001*, pp. 263-268; also *Journal of Electrical & Electronic Engineering Australia*, Vol. 22, No. 1, pp.17-23, 2002.

[3] F. R. Delfeld and G. J. Murphy, "Analysis of Pulse-Width-Modulated Control Systems," *IRE Transactions on Automatic Control*, Vol. 6, No. 3, pp. 283-292, Sep. 1961.

[4] Q. Li and P. Wolfs, "Variable Frequency Control of the Half Bridge Dual Converter," *Proc. AUPEC, 2003*.

[5] P. J. Wolfs, "A Current-Sourced DC-DC Converter Derived via the Duality Principle From the Half-Bridge Converter," *IEEE Trans. Industrial Electronics*, Vol. 40, No. 1, pp. 139-144, Feb. 1993.

[6] C. P. Steinmetz, "On the Law of Hysteresis," *Proc. of the IEEE*, Vol. 72, pp. 196-221, Feb. 1984.

[7] L. H. Mweene, C. A. Wright and M. F. Schlecht, "A 1 kW 500 kHz Front-End Converter for a Distributed Power Supply System," *Proc. IEEE APEC*, 1989, pp. 423-432; also in *IEEE Trans. Power Electronics*, Vol. 6, No. 3, pp. 398-407, Jul. 1991.

[8] S. A. El-Hamamsy and R. A. Fisher, "Inclusion of Nonlinear Output Capacitor Behavior in Zero-Voltage Switched Circuit Design," *Proc. IEEE PESC*, 1997, pp. 1424- 1430.

[9] K. Yao and F. C. Lee, "A Novel Resonant Gate Driver for High Frequency Synchronous Buck Converters," *Proc. IEEE APEC, 2001*, pp. 280-286; also *IEEE Trans. Power Electronics*, Vol. 17, No. 2, pp. 180-186, Mar. 2002.

[10] Q. Li and P. Wolfs, "The Resonant Half Bridge Dual Converter with a Resonant Gate Drive", *Proc. AUPEC, 2003*.

[11] D. Maksimovic, "A MOS Gate Drive with Resonant Transitions," *Proc. IEEE PESC, 1991*, pp. 527 -532.

[12] *LTC1929/LTC1929-PG Datasheet*, Linear Technology Corporation, 1999.

[13] R. D. Middlebrook, "Topics in Multiple-Loop Regulators and Current-Mode Programming," *Proc. IEEE PESC*, 1985, pp. 716-732.